A Model of Fibroblast Motility on Substrates with Different Rigidities

Irina V. Dokukina and Maria E. Gracheva*
Department of Physics, Clarkson University, Potsdam, New York

ABSTRACT To function efficiently in the body, the biological cells must have the ability to sense the external environment. Mechanosensitivity toward the extracellular matrix was identified as one of the sensing mechanisms affecting cell behavior. It was shown experimentally that a fibroblast cell prefers locomoting over the stiffer substrate when given a choice between a softer and a stiffer substrate. In this article, we develop a discrete model of fibroblast motility with substrate-rigidity sensing. Our model allows us to understand the interplay between the cell-substrate sensing and the cell biomechanics. The model cell exhibits experimentally observed substrate rigidity sensing, which allows us to gain additional insights into the cell mechanosensitivity.

INTRODUCTION

It has been established that viable cells sense their mechanical environment along with their biochemical environment, and that, in turn, the mechanical environment regulates cell function (1,2). Cell motility is one of the functions regulated by this extracellular matrix. Cell motility plays an extremely important role in many aspects of life. It is engaged, for example, in such diverse areas as embryonic development, response to infection by the immune system, wound healing, formation of new blood vessels, and in cancer metastasis (3,4).

The majority of earlier experiments on cell motility mechanisms was done on stiff substrates such as glass or plastic, with which cells can form strong attachments (see, for example, (5,6)). These cell-substrate adhesions not only anchor cells but are needed to sustain the forward motion as well. It was found that different types of cells (i.e., fibroblasts (1,7), endothelial cells (8), smooth muscle cells (9), etc.) are able to sense substrate stiffness. In particular, cells cannot form adhesions on soft substrates, and, as a result, they cannot spread and therefore, remain stationary. On very rigid substrates, the opposite situation occurs, and here cells cannot release adhesions. The matrix stiffness also limits myosin II contraction directly, because soft surroundings physically do not support much contraction (10). Thus, cells are able to move only on substrates that have intermediate stiffness, in which cells can effectively grab the surface and detach the rear. Only by this balance, between the cell contractility and the cell-substrate interaction, can cell motion be produced.

It has been shown that cells can also sense rigidity that is gradient in the substrate, and, change speed and direction of motion accordingly. This phenomenon is called ''durotaxis'' (see (2,10) for reviews). The mechanism of durotaxis is not completely understood. According to Lo et al. (1), the main mechanism supporting durotaxis comes from the mechanical feedback from a substrate to a cell, which balances the receptor-ligand complex displacement with the tension at the anchorage site. An additional role in durotaxis is believed to be due to the extracellular calcium influx through stress-activated channels (1).

Bischofs and Schwarz (11), on the other hand, focus on the elastic properties of the extracellular environment, operating under the assumption that cells prefer an environment that supports the most effective application of force. (The particular molecular mechanisms of durotaxis are still intensively discussed; see Giannone and Sheetz (12) for an extended review of the role of different cell proteins in the rigidity sensing.)

Whether cell movement on a substrate is chemically guided, mechanically guided, or both, this guidance is mediated by the cell cytoskeleton. A cell cytoskeleton is made of filaments (F-actin, microtubules, and intermediate filaments) and accessory proteins such as myosin II and integrins, as well as many other proteins and biomolecules. In general, a cell is modeled either as a whole (13,14) or is divided into two main parts: 1), the lamellipodium, and 2), The cell body, where the bulk of cell mass, including nucleus, is contained (15,16).

Several whole-cell computational models which consider molecular mechanisms important for cell motility (such as actin polymerization/depolymerization, integrins, and myosin II dynamics) were developed (13,15,17–19). In addition, the rule-based models that focus on common mechanisms in cell motility also exist (20–22) (for reviews see (23–25)).

Typically, in these models, the cell cytoskeleton is considered as a collection of a small number of nodes, connected by elastic springs and viscous dashpots according to a corresponding viscoelasticity model. Subsequently, the resulting force balance equations are solved at each node. This approach is easily understood, and allows one to study qualitative features of cell motility. Particularly, DiMilla et al. (17) studied a one-dimensional mechanical model of cell locomoting on substrates with different adhesiveness. Mogilner et al.

Submitted April 10, 2009, and accepted for publication March 12, 2010.

*Correspondence: gracheva@clarkson.edu

Editor: Alexander Mogilner.

0006-3495/10/06/2794/10 $2.00

doi: 10.1016/j.bpj.2010.03.026

(26) presented the minimal one-dimensional model of cell locomotion applied to the steady gliding movement of a fish keratocyte. It was demonstrated that the dynamics of actin fiber self-alignment and contraction of the actin-myosin network may explain forward translocation of the cell body.

Bottino (27) developed a mechanical model of cell based on the immersed boundary method. In this method, the actin crosslinks among the actin filament clusters are represented as springs, with the rest lengths depending on local biochemical signal strength. The technique was also applied in Bottino et al. (15) to a two-dimensional model of nematode sperm crawling. Another two-dimensional model in which model cell consisted of uniformly distributed spring-dashpot subunits radiating from the nucleus was proposed in Coskun et al. (28), where an amoeboid cell motility with application to live cell imaging data was studied.

Individual and collective cell movement of *Dictyostelium discoideum* was studied by means of discrete models in Palsson and Othmer (29) and Dallon and Othmer (30). The viscoelastic properties of single cells were taken into account while assuming that cells are deformable ellipsoids, each of which contains a spring in parallel with a Maxwell element.

To produce forward motion, a biological cell utilizes actin polymerization at the leading edge and molecular motors such as myosins to push and pull against the substrate adhesions. Many models consider the leading cell front protrusion to be due to actin polymerization and the action of myosin motors as active forces that should be taken into consideration. Different approaches to specifying cell active forces exist; here we discuss only the most representative of them. If a cell or a lamellipodium is modeled by a set of connected nodes, the active stress (13) or tensile forces (15) can be specified for each pair of connected nodes. Another approach is to apply active forces either to each lamellipodium node (16,31), or only at the front boundary nodes of the lamellipodium (20), and then to define their direction as radiated from the center of the model cell (20). In addition, to specify the direction of the cell motion, either a gradient in active stress due to intracellular molecular processes (13) or a gradient in some external factors, such as in chemotaxis (15), or even a rule based top-down approach, (16,20) is used.

In this article, we focus our attention on model development for a fibroblast cell. The fibroblast is a widely studied cell type. A fibroblast moves using an actin-based cytoskeleton and exhibits stages of locomotion (when moving on a plane substrate) that are common to all motile cells. Relatively simple cytoskeleton organization of fibroblasts with active contractile forces generated mainly at the cell front with the cell rear serving as a passive anchorage (32) allows us to develop a biomechanical model of fibroblast locomotion, incorporating many features from previously developed models (13,15,17).

Recent experiments revealed that fibroblasts planted on the substrate with a step in rigidity show preference for movement on the stiff side of the substrate (1). Here, we present a cell model that is able to interpret these experiments. We base our model assumptions on the experimental observations, omitting the precise details of biomolecular interactions at this time. Our model adequately describes fibroblast motility on substrates with different rigidities. At the same time, the model allows us to make additional predictions that have not yet been studied experimentally.

METHODS

Cell biomechanics

The two-dimensional cell cytoskeleton is modeled by N nodes connected by edges according to the Delaunay triangulation (Fig. 1). We consider the model cell situated on the (x, y) plane with coordinates of the cell nodes denoted as (x_i, y_i). Because experiments revealed the viscoelastic nature of the cell cytoskeleton (24,25), each edge that connects neighboring nodes i and j, consists of a Hookean spring with elasticity coefficient E_{ij} and a dashpot with viscosity coefficient μ, connected in parallel (Fig. 1). At each cell node i, the substrate frictional drag $\vec{F}_i^{\text{drag}}$, passive viscoelastic $\vec{F}_i^{\text{viscoelas}}$, and active $\vec{F}_i$ forces are balanced:

$$\vec{F}_i^{\text{drag}} + \vec{F}_i^{\text{viscoelas}} = \vec{F}_i. \tag{1}$$

Thus, the model cell is described by a set of the following force balance equations for each i^{th} node ($i = 1\ldots N$, $N = 95$) with $j = 1\ldots M_i$ neighbors:

$$\mu_{0i}\frac{\partial \vec{r}_i}{\partial t} + \sum_{j=1}^{M_i}\left(\mu\frac{\partial \varepsilon_{ij}}{\partial t} + E_{ij}\varepsilon_{ij}\right)\hat{r}_{ij} = \vec{F}_i. \tag{2}$$

Here, μ_{0i} is the viscosity coefficient simulating the effective viscous drag force (under i^{th} node) due to the cell-substrate interaction. The expression $\vec{r}_i = (x_i, y_i)$ is the radius-vector of i^{th} node, μ is the cell cytoskeleton viscosity coefficient, and E_{ij} is the cell cytoskeleton elasticity coefficient. The expression ε_{ij} is the linear deformation of the spring between neighboring nodes i and j, $\hat{r}_{ij}$ is the unit vector parallel to the line connecting neighboring nodes i and j, and $\vec{F}_i$ is the active force, modeling myosin II powered contractions and applied at node i. (For a detailed description of all terms in Eq. 2, see the motivation below and the Supporting Material.)

Cell viscoelasticity

Recent experiments indicate a gradual but significant decrease in the elasticity of fibroblast lamellipodium from the leading edge of the cell toward the rear (1,33–35). Hence, we assume that the actin network density, and thus its elasticity, quadratically decreases with position inside the model cell, from its maximum value at the front to the minimum at the rear of the cell. Particularly, we assume that the elasticity coefficient E_{ij} of the cytoskeleton changes from $E_{\max} = 10^{-3}$ kdyn/cm at the cell front to $E_{\min} = 10^{-5}$ kdyn/cm at the cell rear, along the cell, and that it does not change in the direction normal to the cell symmetry axis (Fig. S1 in the Supporting Material).

We choose constant viscosity coefficient $\mu = 0.2 \times 10^{-4}$ kdyn $\times$ min/cm of the cell cytoskeleton. However, the gradient in cell viscosity, as well as other gradients of physical properties of the cell and the substrate (for example, a gradient in the cell-substrate attachment strength), can be readily included in our model.

To compare our model parameters with experimental data (see Table 1), the experimental elasticity and viscosity coefficients should be multiplied by 1 μm $= 10^{-4}$ cm, which is the assumed cell height in our model (36). In general, the cell elasticity coefficient affects the equilibrium length of the cell, whereas the cell viscosity coefficient influences the characteristic

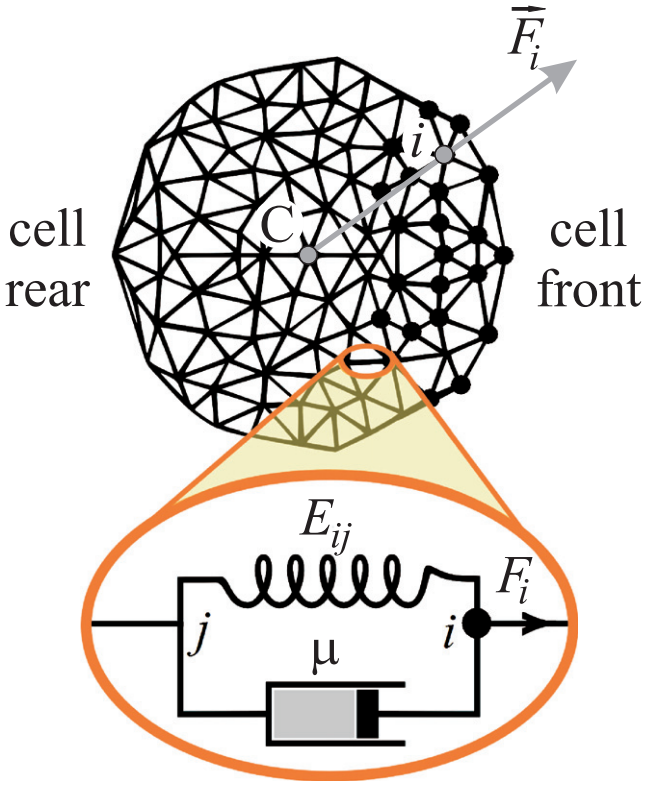

FIGURE 1 Two-dimensional cell mesh and the cytoskeleton mechanical properties. The nonstretched cell is shown at the initial time moment. Each edge that connects neighboring nodes i and j is modeled as an elastic spring with elasticity coefficient E_{ij} and viscous dashpot with viscosity coefficient μ, connected in parallel. The active forces F_i are applied only at the front of the cell, at nodes marked by the large solid dots. A representative force is marked by a shaded arrow. The cell center is indicated by a letter C.

time it takes to stretch or compress the cell. The latter has no significant effect on the phenomena studied in this work. However, the cell viscosity coefficient could be important in producing a specific pattern of traction forces under the cell planted on an elastic substrate.

Cell force generation

Consider a pair of neighboring nodes in the frontal region of the cell. An applied contractile force between such two nodes mimics an acto-myosin fiber connecting them. Assuming that the cell-substrate adhesion is uniform at every node, the local net force at each node (which is a sum of all the contractile forces from the neighboring nodes) should point in the general direction of the cell front, if the cell is to move in the chosen direction. Thus, according to this representation, we simply apply forces at every node radiating toward the cell front. In a more complex case with graded or nonuniform adhesion throughout the cell, the applied local forces could point in various directions (which will also result in a complex pattern of traction forces underneath the cell); however, to produce persistent motion, the overall cell force should again point toward the cell front.

The localization and magnitude of the cell-generated active forces in a model cell should correspond to the specific type of cell that is being simulated. In our fibroblast model, the direction of the active force at each node is determined by extending the line connecting the i^{th} node with the cell center. The direction of the applied force at i^{th} node is indicated by the shaded arrow in Fig. 1. The choice of the point from which the forces radiate (the cell center in our model) is arbitrary; however, such a setup represents the effect of the existing acto-myosin stress fibers that extend throughout the fibroblast cell, mostly between focal adhesions localized at the cell leading edge and the cell body. These focal adhesions also serve as signaling centers and anchor the actin cytoskeleton to the substrate.

We assume that the magnitude of the active force $|F_i|$ is nonzero for nodes marked by the large solid dots in Fig. 1 and Fig. S1, while $|F_i|$ is zero for the rest of the nodes. This is in agreement with the experimentally observed distribution of active forces in fibroblasts, which are mostly found at the cell front (32). In addition, by thus specifying the cell front and rear, we assume our cell to be in a polarized state (37).

It was observed that on softer substrates, a cell produces smaller traction stress, whereas on stiffer substrates the traction stress increases (1). Because cells are able to develop stronger mechanical forces on rigid substrates, it is natural to assume that the active force generated by the cell increases with substrate rigidity. We use a Hill function to describe the active force growth with substrate rigidity. The choice of the Hill function is reasonable, because the growth of the cell-generated active force with the substrate rigidity should be limited by the total amount of the available nonmuscle myosin II in the cell. Thus, the active force should arrive at a plateau once all the myosin motors in the cell are activated. At the same time, because the active force generation by myosin motors in a cell is ultimately coupled (through the actin cytoskeleton) with the cell-substrate attachments, it should be described by a higher order function than a saturation function (see discussion below for the cell-substrate interaction).

This perception also supports the suggestion, frequently discussed in literature (38), that the cell-generated forces are triggered through a molecular or mechanical switch coupled to the substrate properties. Within our model, we are not in a position to resolve which type of switch (molecular or mechanical) it is. However, such a switch will be nonresponsive at low substrate rigidities, fast-reacting near a critical value, and quickly saturate at high rigidities.

Therefore, we use the following dependence of the magnitude of the cell-generated force at i^{th} front node on the substrate rigidity σ_{ST} (Fig. 2),

$$|F_i| = \frac{|F_{\text{act}}|}{N_{\text{front}}} \times \frac{(\sigma_{ST})^2}{(\sigma_{ST})^2 + \sigma_{av}^2}, \tag{3}$$

where $|F_{\text{act}}| = 6$ mdyn is the maximum active force, $\sigma_{av} = 400$ kdyn/cm^2 is the optimal substrate rigidity, and $N_{\text{front}} = 24$ is the number of cell frontal nodes, which are the nodes marked by the large solid dots in Fig. 1. Note that

$$\sigma_{ST} = \sigma_{ST}(x_i, y_i),$$

where (x_i, y_i) are the current coordinates of the i^{th} node on the substrate (see Supporting Material). In our model, the optimal rigidity is the rigidity of the substrate upon which the cell reaches maximum speed of locomotion. In nature, it is the rigidity of the native tissue (extracellular matrix) through which these fibroblast cells are designed to navigate, such as connective or fibrous tissue. The active force $|F_{\text{act}}| = 6$ mdyn $= 60$ nN generated by the cell is the most frequently reported experimentally measured fibroblast force per cell, although values in the range of 0.1–1000 nN were reported (39,40).

TABLE 1 Cell and substrate properties (experimental data)

Definition	Value	Ref.
Cell length	50–70 μm	(1,58)
Substrate rigidity	140–300 kdyn/cm^2	(1)
Force per cell	5×10^{-3}–0.1 dyn	(39,40)
Cell viscosity	0.2–20 kdyn $\times$ min/cm^2	(40)
Cell elasticity	0.001–2.5 $\times$ 10^4 kdyn/cm^2	(39,40)
Cell speed	0.44–0.54 μm/min	(1)
Cell area	1740–2180 μm^2	(1)

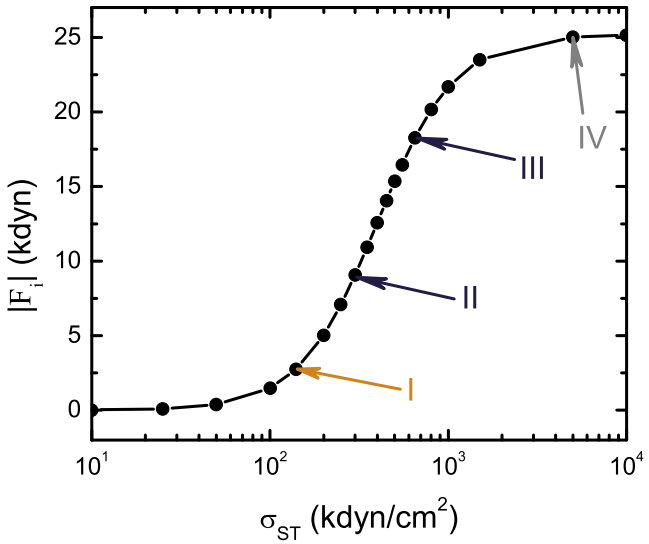

FIGURE 2 The assumed magnitude of cell active force $|F_i|$, at i^{th} node, as a function of the substrate rigidity σ_{ST}. Four considered substrates are marked as I, II, III, and IV. See Table 2 for rigidity values of these substrates.

Cell-substrate interaction

It was found, experimentally, that cells attach better to stiffer materials (7,8,41–43). Moreover, quantitative analysis of experimental data for epithelial cells revealed a linear dependence of the force at a single focal adhesion on substrate rigidity (44). A technological approach, proposed in Saez et al. (44), did not allow to study substrates with rigidities higher than 1000 kdyn/cm^2. However, the authors (44) did expect the attachment force to plateau for very stiff substrates. Note that the rigidity of a bone tissue is of the same order: 1000 kdyn/cm^2 = 100 kPa, which is greater than the rigidity of the native for fibroblast tissues.

For a steady moving cell, the adhesion force is proportional to the cell-substrate viscous interaction, simply described by a viscosity coefficient (multiplied by the cell speed). Thus, we assume that the viscosity coefficient μ_{0i} due to the cell-substrate interaction at the i^{th} node is a linearly increasing function of substrate rigidity,

$$\mu_{0i} = k \times \sigma_{ST}, \tag{4}$$

where $\sigma_{ST} = \sigma_{ST}(x_i, y_i)$ is the substrate rigidity at the i^{th} node with coordinates (x_i, y_i) and $k = 10^{-6}$ min $\times$ cm is the proportionality coefficient. The viscosity coefficient may eventually saturate with substrate rigidity; however, this saturation happens outside of the substrate rigidity range suitable for fibroblasts (44).

See Table 1 for cell and substrate properties known from experiment and Supporting Material for computational details.

RESULTS AND DISCUSSION

Cell speed and cell-substrate contact area as functions of substrate rigidity

The calculated cell speed v (Fig. 3 *a*) is a bell-shaped function of the substrate rigidity σ_{ST}. The values of the calculated steady-state cell speed in the model are in quantitative agreement with experimentally observed values for fibroblasts, which are ~0.5 μm/min (1) (see Table 2). We also find that the cell's projected area increases with substrate rigidity

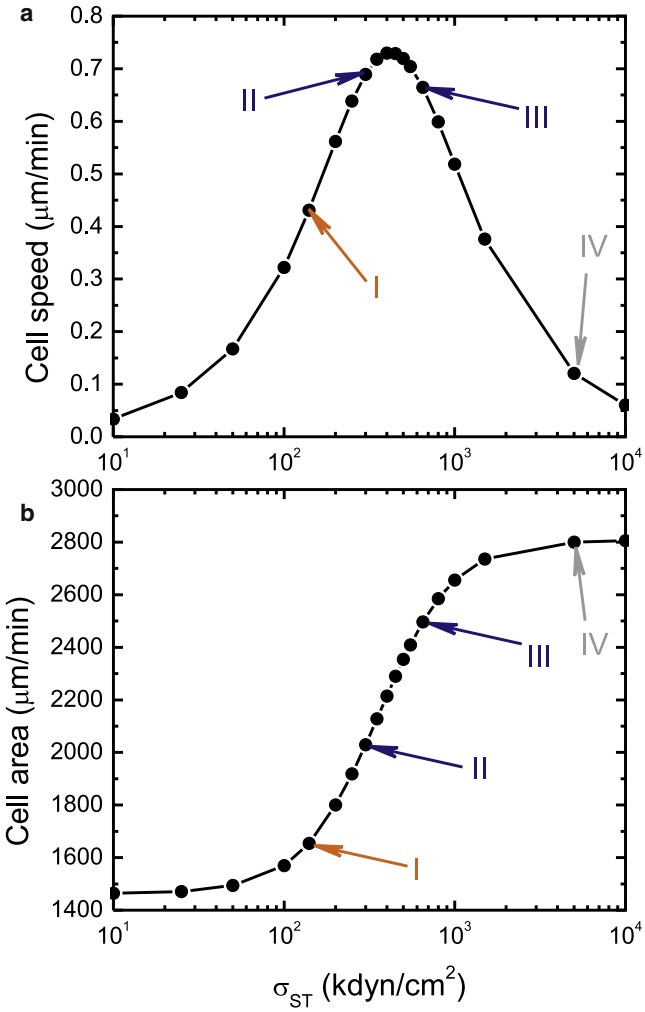

FIGURE 3 (*a*) The calculated steady-state cell speed as a function of substrate rigidity σ_{ST}. The cell moves more efficiently at the intermediate values of substrate rigidity. (*b*) The calculated equilibrium cell area as a function of substrate rigidity σ_{ST}. The model cell has compact shape on soft substrates. This distribution is similar to that seen experimentally (1,8) for fibroblasts. Four considered substrates are marked as I, II, III, and IV.

(Fig. 3 *b*). Indeed, experiments show a general trend toward the growth of projected fibroblast area with the substrate rigidity (1,8,45). The calculated equilibrium cell area is comparable with the observed values (1) for fibroblasts (Table 2).

Previously, similar bell-shaped distribution of cell speed was found experimentally as a function of substrate adhesiveness (46). This dependence was first predicted in DiMilla et al. (17). According to the computational model proposed by DiMilla et al. (17), a biphasic relationship between cell substratum adhesiveness and cell speed arises when bond distribution asymmetry results from a spatial variation in strength of adhesion-receptor/ligand binding. When no difference in adhesiveness exists between the front and rear of the cell, no movement occurs because no asymmetry has been created. Decreasing adhesiveness at the rear (or

TABLE 2 The experimental (1) and calculated cell speed and area on substrates with different rigidities

Substrate rigidity, kdyn/cm^2	Cell speed, μm/min (from (1))	Cell speed, μm/min (this model)	Cell area, μm^2 (from (1))	Cell area, μm^2 (this model)
$\sigma_I = 140$	0.44 ± 0.23	0.43	1740 ± 140	1654
$\sigma_{II} = 300$	0.54 ± 0.13	0.69	2180 ± 170	2028
$\sigma_{III} = 650$	—	0.66	—	2496
$\sigma_{IV} = 5000$	—	0.12	—	2800

increasing adhesiveness at the front) results in a biphasic relationship between movement speed and adhesiveness because bond-number asymmetry has been created (17). Here, the possibility of polarized endocytic trafficking was omitted.

In addition, in the same model, similar effect was observed for the alternative case in which bond-number asymmetry results from polarized receptor recycling, with bond affinity now constant along the cell (17). Again, cell speed can exhibit a biphasic dependence on cell substratum adhesiveness, although for high rates of endocytosis, monophasic behavior develops. Increasing endocytosis rates corresponds to increasing adhesion-receptor number asymmetry between the lamellipod and the uropod (17).

Although DiMilla et al. (17) consider active forces uniformly distributed along the cell, in our model these forces are concentrated at the cell front as was determined for fibroblasts (1). At the same time, in our model the maximum active force generated by the cell grows as a Hill function with substrate stiffness. Contrary to this, in the model of DiMilla et al. (17) there is no postulated dependence of the contractile cell force on substrate adhesiveness. When the level of the cell-generated force in the model of DiMilla et al. (17) is raised, the observed cell speed quickly saturates and becomes independent of the substrate adhesiveness. In our model, the cell speed increases if the cell-generated force grows while cell substrate interaction is kept at a constant level. Increased substrate stiffness hampers this growth, and eventually results in diminished motility.

In previously published models, there was no contractile force asymmetry considered; however, it is natural to assume that, because cell motility results from the balance between the cell-substrate attachment and cell active (contractile and protrusive) force generation, the asymmetry in either of these will result in cell forward motion and a biphasic distribution of cell speed as a function of the cell-substrate adhesiveness. We explored this aspect in Gracheva and Othmer (13).

Ultimately, cell uses the same contractile machinery, the same adhesion mechanisms, and the same signaling pathways to control them regardless of whether it is moving on substrates with different adhesiveness or with different rigidities. Furthermore, we expect to observe similar trends in cellular behavior—in particular, the biphasic cell-speed distribution and saturation in cell elongation as functions of cell-substrate adhesiveness, as observed for Chinese hampster ovarian cells (46) or substrate rigidity, as observed for smooth muscle cells (9). The maximal migration speed of smooth muscle cells occurred on substrates of intermediate rigidity, as observed in Peyton and Putnam (9). Not surprisingly, the precise value of this intermediate rigidity was found to depend on the substrate ligand density. In addition, the ability of cells to form the bundled actin stress-fiber network was found to depend on substrate rigidity (9). A relative absence of these fibers was observed in cells on the softer substrates, in contrast to the well-defined filaments observed in cells on the stiffer substrates (9). This observation also correlates well with our model where active force generated by the cell is a function of the substrate rigidity.

Other experiments also show that the cell speed is reduced on substrates with very large rigidities (2,47). In addition, cells planted on a substrate with gradient in rigidity close to linear, migrate distinctly toward the stiffer region of the substrate, where accumulation of cells occurs (41,48). The accumulation of cells occurs on stiff substrates because the cells move more efficiently on stiff substrates. At the same time, the accumulation of cells becomes less pronounced on the very stiff substrates (49), which is probably due to the significantly reduced cell speed or even inability of cells to move (disengage adhesions) on these substrates. Less-effective cell movement on very stiff substrates was also observed in Peyton and Putnam (9). The biphasic behavior of cell speed on substrate rigidity was also observed for neutrophils, where the optimal motility at intermediate stiffness was also a function of extracellular matrix coating (50).

How does this cellular behavior arise in our model?

As pointed out before, cell motility results from the balance among cell adhesion and cell active and protrusive forces. According to a theoretical estimate (13), the cell speed v depends on the ratio of the active cell force F and the cell-substrate interaction, in our case described by the viscosity coefficient μ_0, as

$$v = F/\mu_0. \tag{5}$$

Both F and μ_0 are assumed to be dependent on substrate rigidity σ_{ST} in our model. In fact, the quantitative behavior (the nonmonotonicity) of cell speed in our model is determined by the particular form of the active force and the viscosity coefficient as functions of substrate rigidity, which are given by Eqs. 3 and 4. We justify these functional dependences as follows.

Both active and drag forces appear to be increasing functions of substrate rigidity within physiological range of tissue rigidities (up to 1000 kdyn/cm^2) (1,42,44). On the other hand, for epithelial cells a linear dependence of the force at a single focal adhesion on substrate rigidity was revealed (44). However, this force may eventually saturate for substrates with very large rigidity (>1000 kdyn/cm^2).

At the same time, increased substrate stiffness is associated with formation of acto-myosin stress fiber bundles (9,51,52), which suggests that the substrate rigidity controls myosin-mediated actin cytoskeleton contractility. The active force in our model is the measure of the cytoskeleton contractility. We assume that the active cell force is a Hill function, meaning that there is an optimal substrate rigidity up to which the cell-generated force is growing rapidly. Once the substrate rigidity is greater than this optimal rigidity, the growth of the cell-generated force slows down and eventually saturates when all of the myosin motors are engaged at very large rigidities. It follows from the experiments (1,9) that the optimal rigidity corresponds to the native rigidity of fibroblast tissues, which is observed to be ~300–400 kdyn/cm^2. This value is smaller than the value of substrate rigidity at which the saturation in cell-substrate interaction (drag force) occurs (1000 kdyn/cm^2). Thus, according to these observations, below the optimal rigidity the active force should increase much more steeply than the drag force, so that the cell speed increases at low rigidity. The maximum cell speed is reached at optimal rigidity due to the fast reacting active force while the drag force is still increasing linearly. At high substrate rigidities, where the active force is at saturation, the drag force keeps on increasing, which results in the cell speed decline.

In addition, because focal adhesions not only anchor the actin cytoskeleton to the substrate or the extracellular matrix, but also have important signaling functions, the value of the optimal rigidity is a function of substrate ligand density (9), which is not considered explicitly in our model. Furthermore, inhibition of ROCK, which is responsible for the bundling of acto-myosin stress fibers, leads to the reduction of cell migration speed in muscle cells on soft and stiff substrates alike (9). In our model, this corresponds to a lower saturation value of the active force generated by the cell, which in turn will result in lower cell speed.

Several theoretical models were put forward in recent years to describe the mechanisms of mechanosensitivity (see (38,42) and references within). One group of models relies on an assumption that focal adhesions, like many other mechanosensing devices in the cell, contain special molecular switches or special proteins that react to the application of force by switching to an active conformation (38). A subgroup of these models proposes that these protein switches sense physical stress (53), while another subgroup suggests that a mechanosensor switch is triggered by local elastic strain (54). There are also models in which the nature of the switch is assumed to be chemical (due to protein signaling (12)). Yet another model does not rely on any hypothetical switches, but maintains that the mechanism of mechanosensitivity is based purely on thermodynamic principles, according to which the stretching stress decreases the protein's chemical potential within the adhesion plaque (55).

Although our model does not discriminate between physical or molecular switching possibly involved in the cell force activation, it does support the presence of a positive feedback between the cell-substrate interaction and the active force generation by the cell. This feedback mechanism is believed to be responsible for reinforcement of the acto-myosin stress fibers (see, for example, (1) or (9)). Given the complexity of cellular responses to extracellular environment, one could conclude that the physical and chemical cues from the substrate act in accordance to produce a specific cellular response.

From soft to stiff: crossing the boundary

To test our model further, we simulate cell motion on substrate with a step in rigidity. It was observed experimentally that fibroblasts can readily cross the boundary on a substrate with a step in rigidity when moving from the soft to the stiff side of the substrate (1). To model the experimental setup from Lo et al. (1), we consider a substrate with a step in rigidity (see the Supporting Material for the description of stiff-soft substrate via a Hill function, which mimics substrate with a step in rigidity). The left-hand side of this substrate has the rigidity σ_{I} and the right-hand side has the rigidity σ_{II} (i.e., soft and stiff, respectively; see Table 2 for the values). We let the model cell move on the soft substrate (σ_{I}) toward the boundary with the stiff substrate (σ_{II}). At the initial time-moment here and below, the cell is located far from the boundary, in order to give it enough time to reach the steady-state speed, equilibrium length, and area that is typical for a given value of σ_{ST}.

Both experimental (Fig. 4 *a*, reproduced from Lo et al. (1) with permission) and simulated (Fig. 4 *b* and Movie S1) cells, initially planted on the soft side of substrate, migrate across the boundary from the soft to the stiff side. Once the model cell migrates to the stiff side of the substrate, its projected area and speed increase until the steady-state is reached (Fig. S2), with the cell shape, as well as the cell speed and area values, that are typical for the stiff substrate. Thus, the model qualitatively describes experimentally observed behavior. The model cell speed and area on both the stiff and the soft substrates are also in good agreement with experiments (see Table 2 for explicit values).

From stiff to soft: turning away from the boundary

Next, we let the model cell move on the stiff side of the substrate (σ_{II}) toward the boundary with the soft side of the substrate (σ_{I}), and with the same step in rigidity.

Both experimental (Fig. 5 *a*, reproduced from Lo et al. (1) with permission) and simulated (see Fig. 5 *b* and Movie S2) cells approaching the boundary from the stiff side do not cross it, but continue to crawl on the stiff side along the boundary. (See Fig. S3 for detailed figures of how the model cell speed and area change during the turn.)

From experimental images, we observe (see Fig. 5 *a*) that the cell approaches the rigidity boundary almost at a 90° angle

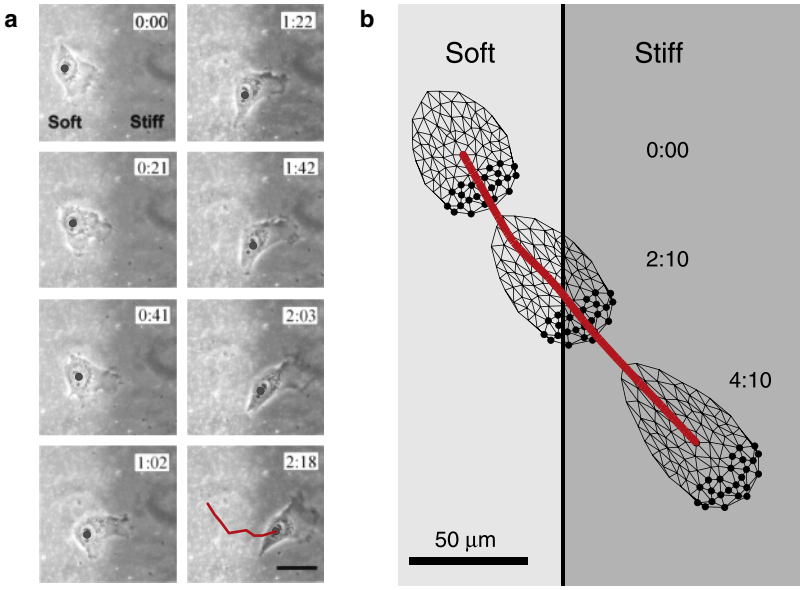

FIGURE 4 (*a*) The fibroblast moves from the soft side of the substrate toward the soft-stiff rigidity boundary and crosses it (reproduced with permission from Lo et al. (1)). Bar, 40 μm. (*b*) The model cell planted on the soft side of the substrate crosses the boundary and continues to move on the stiff side of the substrate. Bar, 50 μm. The trajectory of the cell center is marked with a bold line.

to the boundary (at a normal angle to the boundary), and then changes the direction of motion to move along the boundary. The angle of approach to the stiff-soft substrate boundary is limited in our model. If the model cell path is perpendicular to the boundary, the cell does not ''notice'' the stiff-soft substrate boundary because of the equal active force that the cell generates on the right- and left-hand side of the cell, and the absence of the biochemical regulation of the cell active force as well as of the cell-substrate interaction. As a result, the model cell does not change the direction of movement and crosses the boundary between the two substrate rigidities. There is the critical angle (43.2°) of the cell approach to the rigidity boundary. If the cell approaches the rigidity boundary at an angle between 43.2° and 90°, it makes a mistake and crosses the boundary to the soft side. This angle can be improved by considering wider active cell node distribution throughout the cell or by adding biochemical reactions that will activate forces at dormant nodes during the turn. (See Supporting Material for additional results.) Thus, the dynamic remodeling of acto-myosin fiber distribution is required to capture cell turning behavior at near-normal angles.

To conclude, our biomechanical model not only describes the observed cell speeds and cell spreading tendencies but also captures the essential cell dynamics on substrates with different rigidities, including substrates with the rigidity

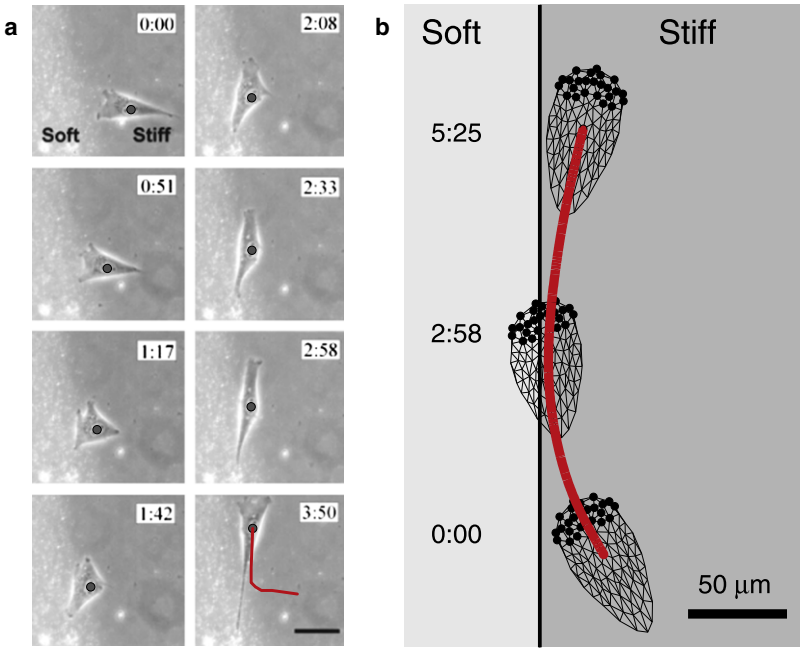

FIGURE 5 (*a*) A fibroblast moves from the stiff side of the substrate toward the stiff-soft rigidity boundary, but does not cross it (reproduced with permission from (reproduced with permission from Lo et al. (1)). Bar, 40 μm. (*b*) The model cell planted on the stiff side of the substrate does not cross the boundary between two rigidities, but turns away from the boundary and stays on the stiff side. Bar, 50 μm. The trajectory of the cell center is marked with a bold line.

step. The suggestion that the substrate contact sites in lamellipodium are stimulated and sustained when they encounter strong mechanical input from a stiffer substrate, which is expressed in Lo et al. (1), falls in line with our model.

A similar idea is expressed in Bischofs and Schwarz (11), who maintain that cells prefer an environment that supports the most effective application of force, at least for fibroblast cells. However, according to our model, even though the cell prefers the environment that supports larger cell forces, the cell motility still can be hampered because of strong cell-substrate adhesion. Additional experiments are required to make certain that this is indeed so. For example, it would be interesting to see a wider range of substrate rigidities studied for one particular set of cells in order to validate our predicted dependence of cell speed on substrate rigidity. It would be useful as well to compare the cell turning behavior between two substrates for a different pair of substrate rigidities, as suggested in an additional discussion found in From Stiff to Very Stiff: The Right-Hand Side of the Bell-Shaped Function (Speed versus σ_{ST}) in the Supporting Material.

CONCLUSIONS

In this work, we have developed a discrete two-dimensional model of cell biomechanics. Our main goal was to study the role of cell mechanics in substrate rigidity sensing, with an emphasis on investigating cell behavior on a substrate that has a rigidity step. We have formulated the observed experimental cell properties as model parameters and did not explicitly consider the biomolecular interactions that lead to these properties. Our model shows how the internal cell mechanics may contribute to experimentally observed cell behavior such as substrate-rigidity sensing.

Even with such a simplified description of a fibroblast cell, we can correctly describe the experimentally observed cellular behavior (1) on a substrate with a rigidity step and make certain predictions. The fibroblasts in the study (1) and the model cell prefer to move on the stiffer substrates. The model cell that moves from the stiff side of the substrate toward the soft side remains on the stiff side, and turns away from the rigidity boundary. The model cell that approaches the boundary from the soft side crosses it and continues to move on the stiff side, similar to the experimentally observed behavior of fibroblasts. The calculated cell speed and cell area are within the experimentally observed range. In addition, the model suggests the bell-shaped dependence of the cell speed to be a function of substrate rigidity.

The model predicts similar cell behavior if the step in rigidity is chosen with rigidity values from the right-hand side of the bell-shaped function $v(\sigma_{ST})$: the cell turns away from the softer substrate and stays on the stiffer substrate if it approaches the boundary between stiff and very stiff substrate rigidities. However, the cell speed will be lower and the cell spread area will be larger in this case. On extremely stiff substrates, the speed of the model cell is so low that the cell can be considered as nonmotile.

Although we apply our model to describe behavior of a fibroblast cell, it may be applied to simulate different types of cells. To do this, we would need to use values of the model parameters corresponding to another cell type, including a specific distribution of active forces in the cell.

A limitation of the model is a notion of a critical angle at which the model cell makes mistakes and chooses the soft substrate over the stiff substrate. This may be corrected by considering the underlying biomolecular processes that are responsible for fast acto-myosin cytoskeleton remodeling and adaptation of cellular processes to the changing extracellular environment.

Future development of the model includes biomolecular regulation of cell active force generation, integrin signaling, and explicit modeling of actin polymerization. A minimal set of biochemical reactions may be modeled that includes conservation of total amount of actin, integrin, and myosin (similar to Gracheva and Othmer (13)). Free diffusion of actin monomers, myosins, and integrins in cytosol, as well as a network-bound actin, acto-myosin complexes, and substrate-bound integrins, could be included. The stochastic approach (56,57) may also be applied to describe the cell-substrate interaction to account for effects due to a finite number of discrete adhesion sites on the substrate, stochastic binding with the substrate, and the variations in the binding strength.

SUPPORTING MATERIAL

One equation, four figures, and three movies are available at http://www.biophysj.org/biophysj/supplemental/S0006-3495(10)00358-9.

We are very grateful to Dr. Yu-Li Wang for the permission to use Fig. 1 *a* and Fig. 1 *b* from Lo et al. (1). We are also grateful to anonymous referees whose comments have allowed us to improve this manuscript.

REFERENCES

1. Lo, C.-M., H.-B. Wang, …, Y. L. Wang. 2000. Cell movement is guided by the rigidity of the substrate. *Biophys. J.* 79:144–152.
2. Discher, D. E., P. Janmey, and Y.-L. Wang. 2005. Tissue cells feel and respond to the stiffness of their substrate. *Science*. 310:1139–1143.
3. Chicurel, M. 2002. Cell biology. Cell migration research is on the move. *Science*. 295:606–609.
4. Bray, D. 2001. Cell Movements: From Molecules to Motility. Garland Publishing, New York.
5. Izzard, C. S., and L. R. Lochner. 1980. Formation of cell-to-substrate contacts during fibroblast motility: an interference-reflection study. *J. Cell Sci.* 80:81–116.
6. Lewis, L., J.-M. Verna, …, E. Bell. 1982. The relationship of fibroblast translocations to cell morphology and stress fiber density. *J. Cell Sci.* 53:21–36.
7. Pelham, Jr., R. J., and Y.-L. Wang. 1997. Cell locomotion and focal adhesions are regulated by substrate flexibility. *Proc. Natl. Acad. Sci. USA*. 94:13661–13665.

8. Yeung, T., P. C. Georges, …, P. A. Janmey. 2005. Effects of substrate stiffness on cell morphology, cytoskeletal structure, and adhesion. *Cell Motil. Cytoskeleton.* 60:24–34.
9. Peyton, S. R., and A. J. Putnam. 2005. Extracellular matrix rigidity governs smooth muscle cell motility in a biphasic fashion. *J. Cell. Physiol.* 204:198–209.
10. Georges, P. C., and P. A. Janmey. 2005. Cell type-specific response to growth on soft materials. *J. Appl. Physiol.* 98:1547–1553.
11. Bischofs, I. B., and U. S. Schwarz. 2003. Cell organization in soft media due to active mechanosensing. *Proc. Natl. Acad. Sci. USA.* 100: 9274–9279.
12. Giannone, G., and M. P. Sheetz. 2006. Substrate rigidity and force define form through tyrosine phosphatase and kinase pathways. *Trends Cell Biol.* 16:213–223.
13. Gracheva, M. E., and H. G. Othmer. 2004. A continuum model of motility in amoeboid cells. *Bull. Math. Biol.* 66:167–193.
14. Paul, R., P. Heil, …, U. S. Schwarz. 2008. Propagation of mechanical stress through the actin cytoskeleton toward focal adhesions: model and experiment. *Biophys. J.* 94:1470–1482.
15. Bottino, D., A. Mogilner, …, G. Oster. 2002. How nematode sperm crawl. *J. Cell Sci.* 115:367–384.
16. Stéphanou, A., E. Mylona, …, P. Tracqui. 2008. A computational model of cell migration coupling the growth of focal adhesions with oscillatory cell protrusions. *J. Theor. Biol.* 253:701–716.
17. DiMilla, P. A., K. Barbee, and D. A. Lauffenburger. 1991. Mathematical model for the effects of adhesion and mechanics on cell migration speed. *Biophys. J.* 60:15–37.
18. Mogilner, A., and D. W. Verzi. 2003. A simple 1-D physical model for the crawling nematode sperm cell. *J. Stat. Phys.* 110:1169–1189.
19. Marée, A. F. M., A. Jilkine, …, L. Edelstein-Keshet. 2006. Polarization and movement of keratocytes: a multiscale modeling approach. *Bull. Math. Biol.* 68:1169–1211.
20. Satulovsky, J., R. Lui, and Y.-L. Wang. 2008. Exploring the control circuit of cell migration by mathematical modeling. *Biophys. J.* 94:3671–3683.
21. Gunji, Y.-P., T. Shirakawa, …, T. Haruna. 2008. Minimal model of a cell connecting amoebic motion and adaptive transport networks. *J. Theor. Biol.* 253:659–667.
22. Zaman, M. H., R. D. Kamm, …, D. A. Lauffenburger. 2005. Computational model for cell migration in three-dimensional matrices. *Biophys. J.* 89:1389–1397.
23. Mogilner, A. 2009. Mathematics of cell motility: have we got its number? *J. Math. Biol.* 58:105–134.
24. Flaherty, B., J. P. McGarry, and P. E. McHugh. 2007. Mathematical models of cell motility. *Cell Biochem. Biophys.* 49:14–28.
25. Lim, C. T., E. H. Zhou, and S. T. Quek. 2006. Mechanical models for living cells—a review. *J. Biomech.* 39:195–216.
26. Mogilner, A., E. Marland, and D. Bottino. 2000. A minimal model of locomotion applied to the steady gliding movement of fish keratocyte cells. *In* Mathematical Models for Biological Pattern Formation. P. K. Maini and H. G. Othmer, editors. Springer, New York.
27. Bottino, D. 2000. Computer simulations of mechanochemical coupling in a deforming domain: application to cell motion. *In* Mathematical Model for Biological Pattern Formation. P. K. Maini and H. G. Othmer, editors. Springer, New York.
28. Coskun, H., Y. Li, and M. A. Mackey. 2007. Amoeboid cell motility: a model and inverse problem, with an application to live cell imaging data. *J. Theor. Biol.* 244:169–179.
29. Palsson, E., and H. G. Othmer. 2000. A model for individual and collective cell movement in *Dictyostelium discoideum*. *Proc. Natl. Acad. Sci. USA.* 97:10448–10453.
30. Dallon, J. C., and H. G. Othmer. 2004. How cellular movement determines the collective force generated by the *Dictyostelium discoideum* slug. *J. Theor. Biol.* 231:203–222.
31. Kuusela, E., and W. Alt. 2009. Continuum model of cell adhesion and migration. *J. Math. Biol.* 58:135–161.
32. Munevar, S., Y.-L. Wang, and M. Dembo. 2001. Distinct roles of frontal and rear cell-substrate adhesions in fibroblast migration. *Mol. Biol. Cell.* 12:3947–3954.
33. Nagayama, M., H. Haga, and K. Kawabata. 2001. Drastic change of local stiffness distribution correlating to cell migration in living fibroblasts. *Cell Motil. Cytoskeleton.* 50:173–179.
34. Laurent, V. M., S. Kasas, …, J. J. Meister. 2005. Gradient of rigidity in the lamellipodia of migrating cells revealed by atomic force microscopy. *Biophys. J.* 89:667–675.
35. Kuznetsova, T. G., M. N. Starodubtseva, …, R. I. Zhdanov. 2007. Atomic force microscopy probing of cell elasticity. *Micron.* 38: 824–833.
36. Revell, C. M., J. A. Dietrich, …, K. A. Athanasiou. 2006. Characterization of fibroblast morphology on bioactive surfaces using vertical scanning interferometry. *Matrix Biol.* 25:523–533.
37. Ridley, A. J., M. A. Schwartz, …, A. R. Horwitz. 2003. Cell migration: integrating signals from front to back. *Science.* 302:1704–1709.
38. Bershadsky, A., M. Kozlov, and B. Geiger. 2006. Adhesion-mediated mechanosensitivity: a time to experiment, and a time to theorize. *Curr. Opin. Cell Biol.* 18:472–481.
39. Wakatsuki, T., M. S. Kolodney, …, E. L. Elson. 2000. Cell mechanics studied by a reconstituted model tissue. *Biophys. J.* 79:2353–2368.
40. Thoumine, O., and A. Ott. 1997. Time scale dependent viscoelastic and contractile regimes in fibroblasts probed by microplate manipulation. *J. Cell Sci.* 110:2109–2116.
41. Hadjipanayi, E., V. Mudera, and R. A. Brown. 2009. Guiding cell migration in 3D: a collagen matrix with graded directional stiffness. *Cell Motil. Cytoskeleton.* 66:121–128.
42. Schwartz, U. 2007. Soft matters in cell adhesion: rigidity sensing on soft elastic substrates. *Soft Matter.* 3:263–266.
43. Choquet, D., D. P. Felsenfeld, and M. P. Sheetz. 1997. Extracellular matrix rigidity causes strengthening of integrin-cytoskeleton linkages. *Cell.* 88:39–48.
44. Saez, A., A. Buguin, …, B. Ladoux. 2005. Is the mechanical activity of epithelial cells controlled by deformations or forces? *Biophys. J.* 89:L52–L54.
45. Solon, J., I. Levental, …, P. A. Janmey. 2007. Fibroblast adaptation and stiffness matching to soft elastic substrates. *Biophys. J.* 93:4453–4461.
46. Palecek, S. P., J. C. Loftus, …, A. F. Horwitz. 1997. Integrin-ligand binding properties govern cell migration speed through cell-substratum adhesiveness. *Nature.* 385:537–540.
47. Zaman, M. H., L. M. Trapani, …, P. Matsudaira. 2006. Migration of tumor cells in 3D matrices is governed by matrix stiffness along with cell-matrix adhesion and proteolysis. *Proc. Natl. Acad. Sci. USA.* 103:10889–10894.
48. Zaari, N., P. Rajagopalan, …, J. Y. Wong. 2004. Photopolymerization in microfluidic gradient generators: microscale control of substrate compliance to manipulate cell response. *Adv. Mater.* 16:2133–2137.
49. Kuntanawat, P., C. D. W. Wilkinson, and M. O. Riehle. 2007. Cell response to wedge hydrogel on glass substrate as a continuous gradient of stiffness. *In* 9th Meeting of the Surface Science of Biologically Important Interfaces Group. University of Manchester, Manchester, UK.
50. Stroka, K. M., and H. Aranda-Espinoza. 2009. Neutrophils display biphasic relationship between migration and substrate stiffness. *Cell Motil. Cytoskeleton.* 66:328–341.
51. Schlunck, G., H. Han, …, F. Grehn. 2008. Substrate rigidity modulates cell matrix interactions and protein expression in human trabecular meshwork cells. *Invest. Ophthalmol. Vis. Sci.* 49:262–269.
52. Ulrich, T. A., E. M. de Juan Pardo, and S. Kumar. 2009. The mechanical rigidity of the extracellular matrix regulates the structure, motility, and proliferation of glioma cells. *Cancer Res.* 69:4167–4174.

53. Bruinsma, R. 2005. Theory of force regulation by nascent adhesion sites. *Biophys. J.* 89:87–94.

54. Nicolas, A., B. Geiger, and S. A. Safran. 2004. Cell mechanosensitivity controls the anisotropy of focal adhesions. *Proc. Natl. Acad. Sci. USA.* 101:12520–12525.

55. Shemesh, T., B. Geiger, …, M. M. Kozlov. 2005. Focal adhesions as mechanosensors: a physical mechanism. *Proc. Natl. Acad. Sci. USA.* 102:12383–12388.

56. Gillespie, D. 1977. Exact stochastic simulation of coupled chemical reactions. *J. Phys. Chem.* 81:2340–2361.

57. Gracheva, M. E., R. Toral, and J. D. Gunton. 2001. Stochastic effects in intercellular calcium spiking in hepatocytes. *J. Theor. Biol.* 212: 111–125.

58. Munevar, S., Y.-L. Wang, and M. Dembo. 2001. Traction force microscopy of migrating normal and H-Ras transformed 3T3 fibroblasts. *Biophys. J.* 80:1744–1757.